Metabolomics (2019) 15:36
https://doi.org/10.1007/s11306-019-1485-6

ORIGINAL ARTICLE

Peroxisome proliferator-activated receptor A/G reprogrammes metabolism associated with lipid accumulation in macrophages

Guozhu Ye[1,2] · Han Gao[2,3] · Yi Lin[2] · Dongxiao Ding[2,3] · Xu Liao[2] · Han Zhang[2] · Yulang Chi[2] · Sijun Dong[1,2,4]

Received: 13 October 2018 / Accepted: 31 January 2019 / Published online: 4 March 2019

Abstract

Introduction Macrophage metabolism contributes to the progression of metabolic diseases, and peroxisome proliferator-activated receptors (PPARs) play vital roles in macrophage metabolism and the treatment of metabolic diseases. However, the role of PPARs in metabolic reprogramming related to lipid accumulation in macrophages, a key pathological event in metabolic diseases, remains unclear.

Objectives We aimed to identify PPAR-mediated metabolic reprogramming and potential therapeutic targets associated with lipid accumulation in macrophages.

Methods Following treatment with oleate, oleate + WY-14643 and oleate + pioglitazone to induce alterations in PPAR signaling, lipids and relevant metabolism, macrophage samples were analyzed employing an untargeted metabolomics based on gas chromatography–mass spectrometry.

Results The metabolomics approach revealed that multiple metabolic pathways were altered during lipid accumulation in oleate-treated macrophages and responsive to WY-14643 and pioglitazone treatment. Notably, levels of most metabolites involved in amino acid metabolism and nucleotide metabolism were accumulated in oleate-treated macrophages, and these effects were alleviated or abolished by PPARA/G activation. Additionally, during oleate-induced lipid accumulation and lipid lowering with WY-14643 and pioglitazone in macrophages, levels of most amino acids were positively associated with neutral lipid, total cholesterol, cholesterol ester, total free fatty acid and triglyceride levels but negatively associated with expression of genes related to PPARA/G signaling. Furthermore, glycine was found to be a potential biomarker for assessing lipid accumulation and the lipid-lowering effects of PPARA/G in oleate-treated macrophages.

Conclusion The results of this study revealed a high correlation of amino acid metabolism with lipid accumulation and the lipid-lowering effects of PPARA/G in macrophages.

Keywords Peroxisome proliferator-activated receptor · Macrophage · Metabolic reprogramming · Lipid accumulation · Amino acid · Nucleotide

Abbreviations

PPAR	Peroxisome proliferator-activated receptor
FFA	Free fatty acid
GC–MS	Gas chromatography–mass spectrum
DMSO	Dimethyl sulfoxide
DMEM	Dulbecco's modified Eagle medium

Guozhu Ye and Han Gao have contributed equally to this work.

Electronic supplementary material The online version of this article (https://doi.org/10.1007/s11306-019-1485-6) contains supplementary material, which is available to authorized users.

✉ Guozhu Ye
gzye@iue.ac.cn

✉ Sijun Dong
sjdong@iue.ac.cn

[1] Center for Excellence in Regional Atmospheric Environment, Institute of Urban Environment, Chinese Academy of Sciences, 1799 Jimei Road, Xiamen 361021, China

[2] Key Laboratory of Urban Environment and Health, Institute of Urban Environment, Chinese Academy of Sciences, 1799 Jimei Road, Xiamen 361021, China

[3] University of Chinese Academy of Sciences, 19 Yuquan Road, Beijing 100049, China

[4] Institute of Urban Environment, Chinese Academy of Sciences, 1799 Jimei Road, Xiamen 361021, China

PBS	Phosphate-buffered saline
RT-PCR	Reverse transcription-polymerase chain reaction
QC	Quality control
TG	Triglyceride
CE	Esterified cholesterol
TC	Total cholesterol
LDL	Low density lipoprotein

1 Introduction

Metabolic diseases such as obesity, diabetes and atherosclerosis have caused a tremendous health burden globally (Barquera et al. 2015; Bastien et al. 2014; Bhupathiraju and Hu 2016; Piche et al. 2018; Zheng et al. 2018). The incidence rate of obesity has increased in the past few decades, with more than 35% of women and 30% of men worldwide being affected (Bastien et al. 2014; Piche et al. 2018), and approximately one in 11 adults suffers from diabetes (Zheng et al. 2018). Notably, obesity and diabetes contribute to atherosclerotic cardio-cerebral vascular disease, which are the primary illnesses and causes of mortality worldwide (Barquera et al. 2015). Therefore, effective treatment of obesity, diabetes and cardio-cerebral vascular diseases is of great importance.

Macrophages are innate immune cells that reside in many tissues, such as skeletal muscle, liver, adipose and vascular tissues. Signals in obese, diabetic and atherosclerotic microenvironments, such as inflammatory factors, oxidative stress, and excessive nutrient availability, affect macrophage metabolism, which in turn controls its functionality (Appari et al. 2018; Geeraerts et al. 2017; O'Neill and Pearce 2016). For instance, inflammation and oxidative stress accelerate lipid accumulation in macrophages, promoting inflammation and oxidative stress. Moreover, macrophage metabolism has been proposed as an ideal therapeutic target for obesity, diabetes and atherosclerosis, which in macrophages are associated with metabolic disturbances in lipids, amino acids, intermediates in tricarboxylic acid cycle, carbohydrates, nucleotides, and other metabolites (Geeraerts et al. 2017; Kaplan et al. 2012; Mathis and Shoelson 2011; Olefsky and Glass 2010). Accordingly, mediating macrophage functions by reprogramming metabolism would be beneficial for treating obesity, diabetes and cardiovascular disease. Thus, uncovering the metabolic reprogramming and potential therapeutic targets associated with lipid accumulation in macrophages, a key pathological event in obesity, diabetes and cardiovascular disease, is crucial.

Peroxisome proliferator-activated receptors (PPARs) have vital roles in lipid metabolism (such as lipogenesis, lipolysis, lipid transport and oxidation), amino acid metabolism, gluconeogenesis, ketogenesis and other metabolic processes and have great potential for the treatment of obesity, diabetes, atherosclerosis and other metabolic diseases (Kersten et al. 2001; Mandard et al. 2004; Willson et al. 2001). Nonetheless, the molecular mechanism by which PPARs mediate metabolic reprogramming associated with lipid accumulation in macrophages remains unclear. In this study, oleate, a prominent dietary and serum free fatty acid (FFA), was used to suppress the activity of PPARs and induce lipid accumulation in macrophages. Because WY-14643 and pioglitazone, specific agonist for PPARA and PPARG, respectively, are widely used for the treatment of diabetes and cardiovascular disease, macrophages were treated with oleate plus WY-14643 or pioglitazone to activate PPARA/G and abolish lipid accumulation. An untargeted metabolomics approach employing gas chromatography–mass spectrum (GC–MS) was then employed to discover PPARA/G-mediated metabolic reprogramming and potential therapeutic targets associated with lipid accumulation and lipid-lowering effects of PPARA/G in oleate-treated macrophages. To the best of our knowledge, this is the first report that levels of most amino acids and nucleotides increases during lipid accumulation and that these effects can be alleviated or even abolished by PPARA/G activation. Moreover, the results show that glycine can be used as a potential biomarker for assessing lipid accumulation and the lipid-lowering effects of PPARA/G in macrophages treated with oleate.

2 Materials and methods

2.1 Materials

Dimethyl sulfoxide (DMSO, ≥ 99.7%), oleic acid (99.0%), resveratrol (99.0%), WY-14643, pioglitazone, methoxyamine hydrochloride (98%), pyridine (99.8%), and *N*-methyl-*N*-(trimethylsilyl)-trifluoroacetamide (≥ 98.5%) were purchased from Sigma-Aldrich (Shanghai, China). Primers and high-glucose Dulbecco's modified Eagle medium (DMEM) were gained from HyClone (USA) and Shanghai Sangon Biotech (Shanghai, China), respectively. RAW264.7 macrophages were obtained from Cell Bank of Chinese Academy of Science (Shanghai, China).

2.2 Cell culture and treatments

RAW264.7 cells were grown in DMEM medium (high glucose) supplemented with 10% fetal bovine serum at 37 °C in a humidified atmosphere with 5% CO_2. Macrophages were treated with 65 μg/ml oleate for 24 h to suppress PPAR activity and to induce metabolic disorders associated with lipid accumulation. Macrophages were also treated with 65 μg/ml oleate plus 1.5 μg/ml WY-14643, or 65 μg/ml oleate plus 1.5 μg/ml pioglitazone for 24 h to activate PPAR activity and

to reprogramme metabolism associated with lipid accumulation. DMSO (v/v, 1‰) was used as the control.

2.3 Nile red staining

Following fixing in 4% paraformaldehyde for 40 min, macrophages were washed 3 times with phosphate-buffered saline (PBS) and stained with 2.5 μg/ml DAPI (4′,6-diamidino-2-phenylindole, in methanol) for 15 min at 37 °C, followed by washing twice with methanol. Macrophages were then stained with 10 μg/ml Nile red (in methanol) for 0.5 h at 37 °C prior to being washed with PBS. A confocal microscope (LSM 7100, Zeiss, Germany) was used for confocal fluorescence imaging. The Nile red/DAPI ratio was used to determine the cellular neutral lipid content.

2.4 RNA extraction for reverse transcription-polymerase chain reaction (RT-PCR) analysis

Total RNA from macrophages was extracted using TRIzol reagent (Thermo Fisher Scientific, MA, USA). Reverse transcription to cDNA was performed with PrimeScript™ RT master mix (Takara, Dalian, China). Real-time RT-PCR was performed using SYBR® Premix Ex Taq™ II (Takara, Dalian, China). β-Actin was used as the internal standard to normalize gene expression using the $2^{-\Delta\Delta Ct}$ method. For quantitative PCR analysis, primers were designed according to the NCBI database (Table S1).

2.5 Sample collection and preparation for metabolomics

After cell culture and treatments, macrophages were rinsed with PBS and then collected using a scraper. The cells were centrifuged for 5 min at 5000 rpm and frozen in liquid nitrogen prior to storage at − 80 °C for subsequent sample preparation. The cell sample was mixed with 1000 μl of 80% ice-cold methanol and vortexed for 1 min, and the cells were centrifuged at 4 °C for 15 min at 13,000 rpm. The supernatant (800 μl) was collected into a 1.5-ml centrifuge tube and dried using a SpeedVac concentrator (Thermo Scientific, USA). The dried sample was dissolved in 50 μl of 20 mg/ml methoxyamine hydrochloride (in pyridine) and vortexed for 30 s prior to the oximation reaction in a water bath at 37 °C for 1.5 h. The sample was mixed with 40 μl of *N*-methyl-*N*-(trimethylsilyl)-trifluoroacetamide and vortexed for 10 s, followed by the silylation reaction in a water bath at 37 °C for 1.0 h. Following centrifugation at 4 °C for 15 min at 13,000 rpm, the supernatant of the derivatized sample was injected for subsequent instrumental analysis. To monitor the repeatability and stability of the metabolomics approach, the residual supernatants of all samples were mixed thoroughly and divided into 800-μl aliquots as quality control (QC) samples. One QC sample was processed every 6 analytical samples under the same parameters as the other samples with respect to vacuum drying, derivatization, instrumental analysis and data processing.

2.6 Instrumental analysis for metabolomics

A GC-MS system (GCMS-QP 2010 plus, Shimadzu, Japan) equipped with an AOC-20i autosampler was employed to acquire metabolic profiles of the cell samples. The parameters were similar to those utilized in our previous studies (Shao et al. 2018; Ye et al. 2014, 2012). Injection volume was 1 μl. Metabolites were separated using a DB-5 MS capillary column (30 m × 250 μm × 0.25 μm, J&W Scientific Inc., USA). The carrier gas (helium) was used in constant flow mode. The linear velocity of helium and the split ratio were set to 40.0 cm/s and 2:1, respectively. The oven temperature was kept at 70 °C for 3.0 min, increased to 300 °C at a rate of 5 °C/min, and then held at 300 °C for 10 min. The temperatures of the interface, ion source and inlet were set to 280, 230 and 300 °C, respectively. Metabolites were ionized by electron impact (70 eV). The detector voltage was set in line with the tuning results. GCMS solution 2.7 (Shimadzu, Japan) was used to acquire mass signals (m/z, 33–600) in full scan mode. The solvent delay time was 5.5 min, and the event time was 0.2 s. The retention time of *n*-alkanes was obtained by analyzing a light diesel sample in the same way as the analytical samples, which was then used to calculate the retention indices for the metabolites.

2.7 Data preprocessing for metabolomics

Following transformation into NetCDF format by GCMS solution 4.2 (Shimadzu, Japan), raw mass data were applied for peak matching employing XCMS (Smith et al. 2006). The signal-to-noise ratio was 3 in the process of peak matching. Feature ions of the metabolites were generated after deconvolution of the mass signals using ChromaTOF 4.43 (LECO Corporation, USA). Metabolite identification was performed mainly based on both automatic and manual spectral comparisons and further verified by available reference standards according to the mass spectra, retention time and retention indices. The ion peak area of the metabolite was normalized to total peak areas of all metabolites and multiplied by 1×10^8, the data were then applied in the metabolomics analysis.

2.8 Determination of total FFAs and triglycerides (TGs)

After washing with cold PBS, macrophages were harvested using a scraper. Following centrifugation at 4 °C for 5 min

at 2500 rpm, intracellular total FFA contents in the pellets from 80% of the harvested cells were determined using a Free Fatty Acid Quantification Assay Kit (Abcam) according to the manufacturer's instructions. The protein level in 20% of the harvested cells was measured to normalize the total FFA level. Similar to the total FFA measurement, intracellular TG levels in 80% of the harvested cells were measured using a Triglyceride Quantification Assay Kit (Abcam) based on the instructions. Twenty percent of the harvested cells were collected to measure the protein level used for TG normalization.

2.9 Determination of free, esterified (CE) and total cholesterol (TC) levels

Levels of total and free cholesterol were determined using a Cholesterol/Cholesteryl Ester Quantitation Assay kit (Abcam). The protein content was employed to normalize the cholesterol level based on the manufacturer's instructions. CE contents were obtained by subtracting free cholesterol from TC.

2.10 Statistical analysis

MetaboAnalyst 3.0 was applied to perform principal component analysis and pathway analysis (Xia et al. 2015). A two-tailed Mann–Whitney *U* test was performed in MeV 4.9.0 to evaluate differences in metabolite levels among groups (Saeed et al. 2006). An independent sample *t*-tests was conducted using Statistics 18 (SPSS Inc., Chicago, USA) to assess differences in mRNA expression levels and fluorescence intensity among groups. Bivariate correlations among levels of metabolites, total FFAs, TGs, TC, CE, neutral lipids and genes related to PPARA/G signaling were assessed using Pearson correlation coefficients with PASW Statistics 18. The level of statistical significance was 0.05. The heat map was produced using MeV 4.9.0. A binary logistic regression model was constructed to evaluate lipid accumulation and the lipid-lowering effects of PPARA/G using PASW Statistics 18.

3 Results and discussion

3.1 PPARA/G reprogrammes metabolic profiles associated with lipid accumulation in macrophages

We found that the mRNA expression levels of genes involved in PPARA/G signaling, such as *Ppara, Pparg, Rxra, Rxrg, Ppargc1a* and *Lxra*, were significantly inhibited by oleate in macrophages, indicating that oleate suppressed PPARA/G signaling in these cells (Fig. 1a). In addition, the oleated-induced decreases in the mRNA levels of genes related to PPARA signaling including *Ppara, Rxra, Ppargc1a* and *Lxra*, in macrophages, were abrogated by WY-14643; however, the decreases in *Ppara* and *Rxra* mRNA expression in oleate-treated macrophages were not abolished by pioglitazone (Fig. 1a). Moreover, the decreases in mRNA levels of PPARG signaling-related genes, such as *Pparg, Rxrg, Ppargc1a* and *Lxra*, in macrophages caused by oleate were eliminated by pioglitazone, whereas decreases in *Pparg* and *Rxrg* mRNA expression in macrophages treated with oleate were not abolished by WY-14643 (Fig. 1a). Conversely, *Pparb* and *Rxrb* mRNA expression levels were not significantly altered in response to treatment with oleate, oleate plus WY-14643, or oleate plus pioglitazone (Fig. 1a). These data illustrated the high specificity of WY14643 and pioglitazone for activating PPARA and PPARG signaling, respectively.

Nile red staining showed that oleate triggered significant accumulation of neutral lipids in RAW264.7 macrophages and that this accumulation was abolished by both WY-14643 and pioglitazone (Fig. 1b). Furthermore, we observed that contents of major components of neutral lipids, including total FFAs, TGs, TC and CE, were significantly increased by oleate, and these effects were significantly attenuated by both WY-14643 and pioglitazone. Subsequently, an untargeted metabolomics approach using GC–MS was used to reveal PPARA/G-mediated metabolic reprogramming as well as potential therapeutic targets related to lipid accumulation and the lipid-lowering effects of PPARA/G in macrophages. Plotting of principal component analysis scores illustrated that three QC samples clustered together, demonstrating high stability and reproducibility of the metabolomics approach (Fig. 1d). Additionally, we found that the metabolic profile of macrophages treated with oleate differed greatly from that of control macrophages and that PPARA/G activation induced significant alterations in the metabolic profiles of oleate-treated macrophages (Fig. 1e). These data indicate that significant metabolic alterations occurred during lipid accumulation and PPARA/G activation.

3.2 PPARA/G reprogrammes metabolism associated with lipid accumulation in macrophages

In total, 84 differential metabolites were identified from comparisons between control, oleate, oleate plus WY-14643, and oleate plus pioglitazone groups, as depicted in a heat map (Fig. 2). The levels of metabolites involved in amino acid metabolism, lipid metabolism, nucleotide metabolism, carbohydrate metabolism and other metabolic pathways were significantly altered in macrophages treated with oleate, oleate plus WY-14643, and oleate plus pioglitazone. Notably, the levels of most metabolites involved in amino acid metabolism and

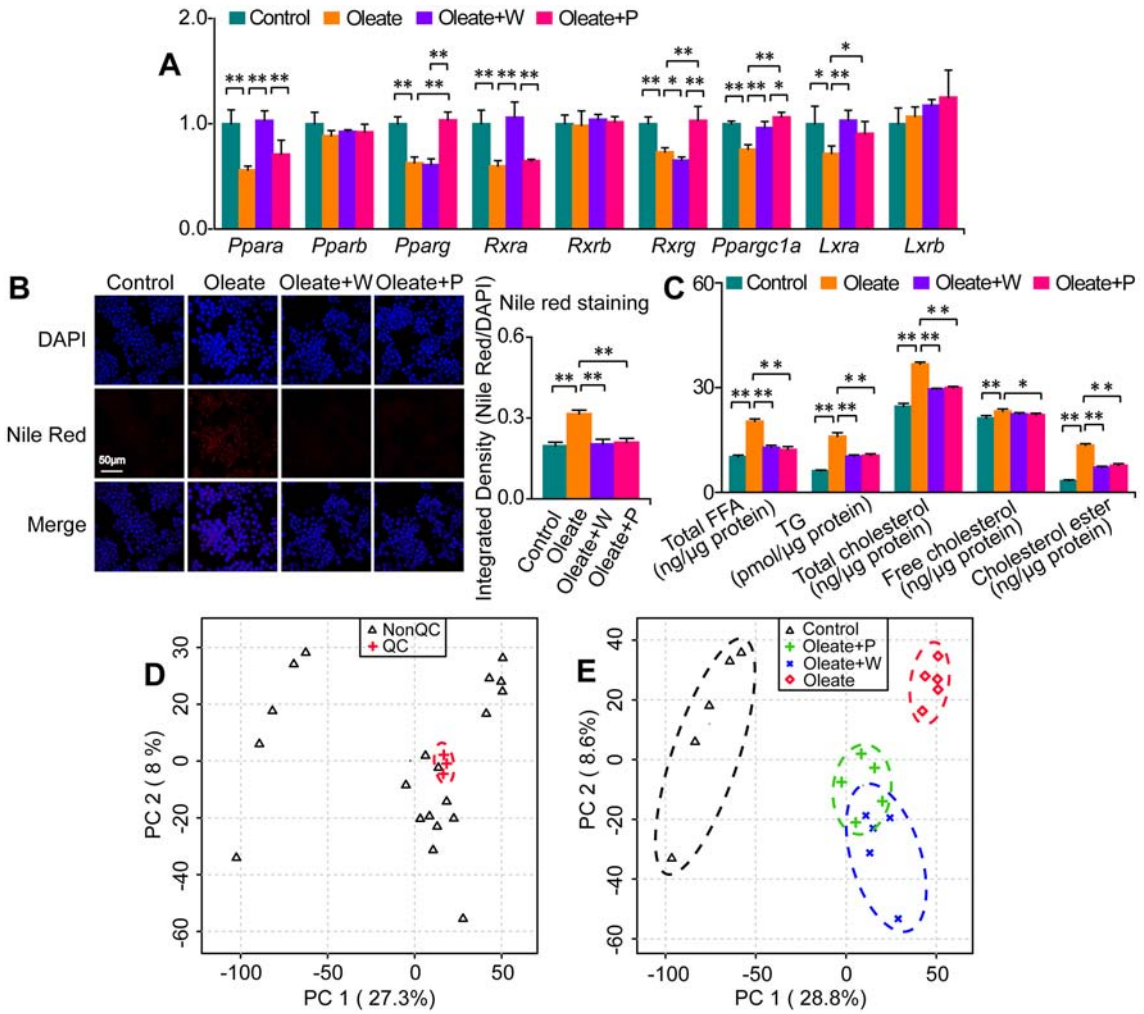

Fig. 1 PPARA/G reprogrammed metabolic profiles associated with lipid accumulation in macrophages. W, WY-14643. P, pioglitazone. Columns represent the mean + SD. *p < 0.05, **p < 0.01, independent samples *t*-test. Changes in PPARA/G signaling (**a**, n = 4 per group), neutral lipids (**b**, n = 9 per group), and major components of neutral lipids (**c**, n = 4 per group) in macrophages treated with oleate, oleate + W, and oleate + P. **d** Analytical performance of the metabolomics approach. **e** Changes in metabolic profiles in macrophages treated with oleate, oleate + W, and oleate + P. n = 5 per group

nucleotide metabolism were significantly increased in macrophages treated with oleate, and these increases induced by oleate were attenuated or abolished by PPARA/G activation. Further pathway analysis showed that 43 metabolic pathways were disturbed in macrophages treated with oleate and that 33 and 36 metabolic pathways were responsive to PPARA/G activation, respectively (Fig. 3). PPARs are revealed to be involved in amino and bile acid metabolism, lipoprotein, mitochondrial and peroxisomal FFA oxidation, microsomal FFA hydroxylation, gluconeogenesis, ketogenesis, biotransformation and other metabolic pathways (Mandard et al. 2004). Notably, intermediates in PPAR-mediated metabolic pathways could be transformed into each other to fulfill specific cellular functions. Details regarding the metabolic reprogramming regulated by PPARA/G are provided below.

3.3 PPARA/G reprogrammes amino acid metabolism associated with lipid accumulation in macrophages

Amino acids can be utilized for energy production, and synthesis of proteins, lipids and nucleotides to support cell proliferation and growth. PPARs mediate the expression levels of many genes related to amino acid metabolism, such as those involved in deamination, transamination, amino acid inter-conversions, alpha-keto acid oxidation, and production of amino acid derivatives (Kersten et al. 2001). In the present study, we found that PPARA/G signaling was significantly inhibited and that the levels of most metabolites involved in amino acid metabolism were significantly increased in macrophages treated with oleate (Figs. 1, 4a). Moreover, such oleate-induced increases in

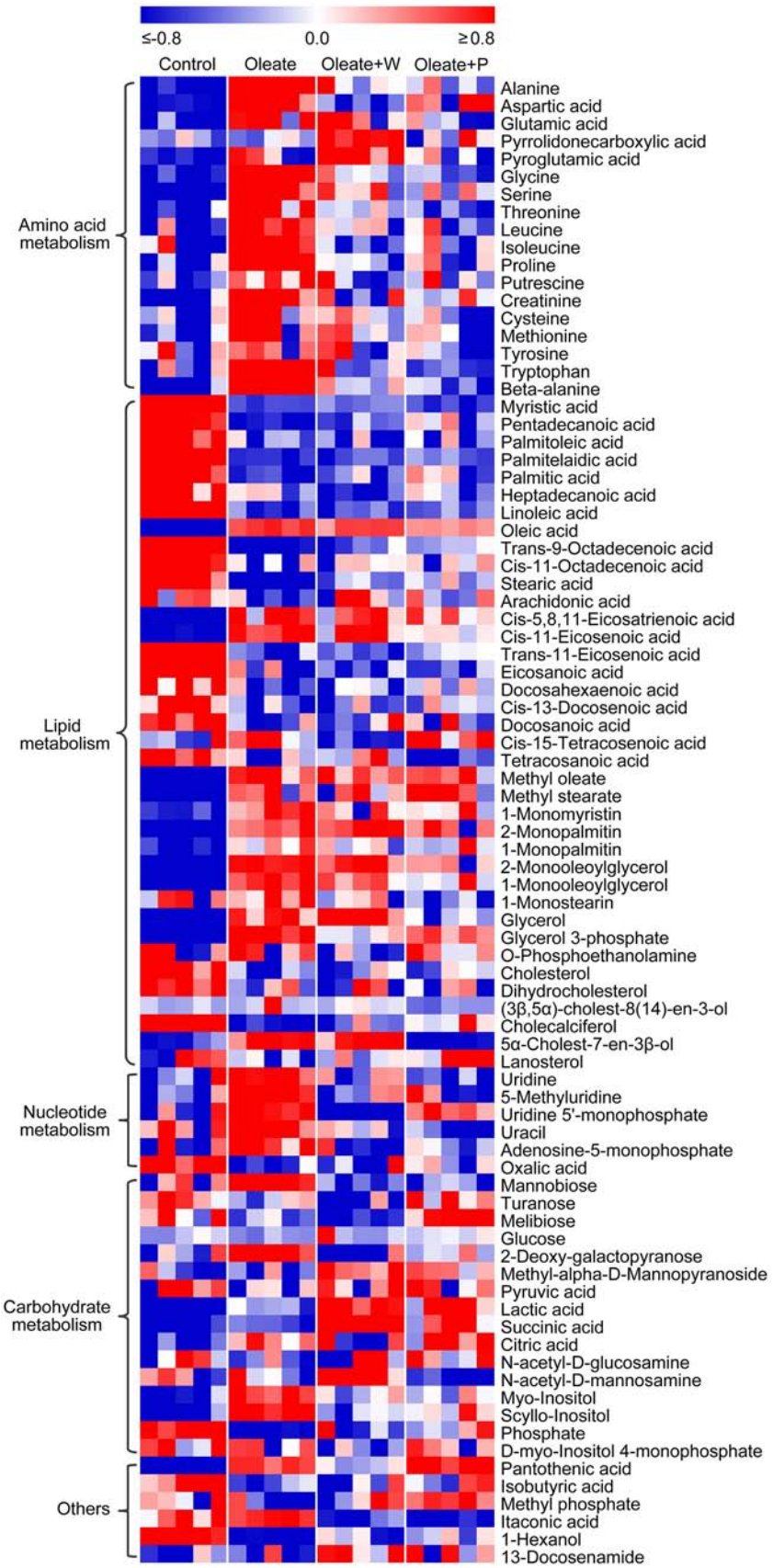

Fig. 2 Heat map of metabolic changes in macrophages treated with oleate, oleate plus WY-14643 (W), and oleate plus pioglitazone (P). The contents of metabolites were divided by the standard deviation after subtracting the mean, and the data were then employed to generate the heat map

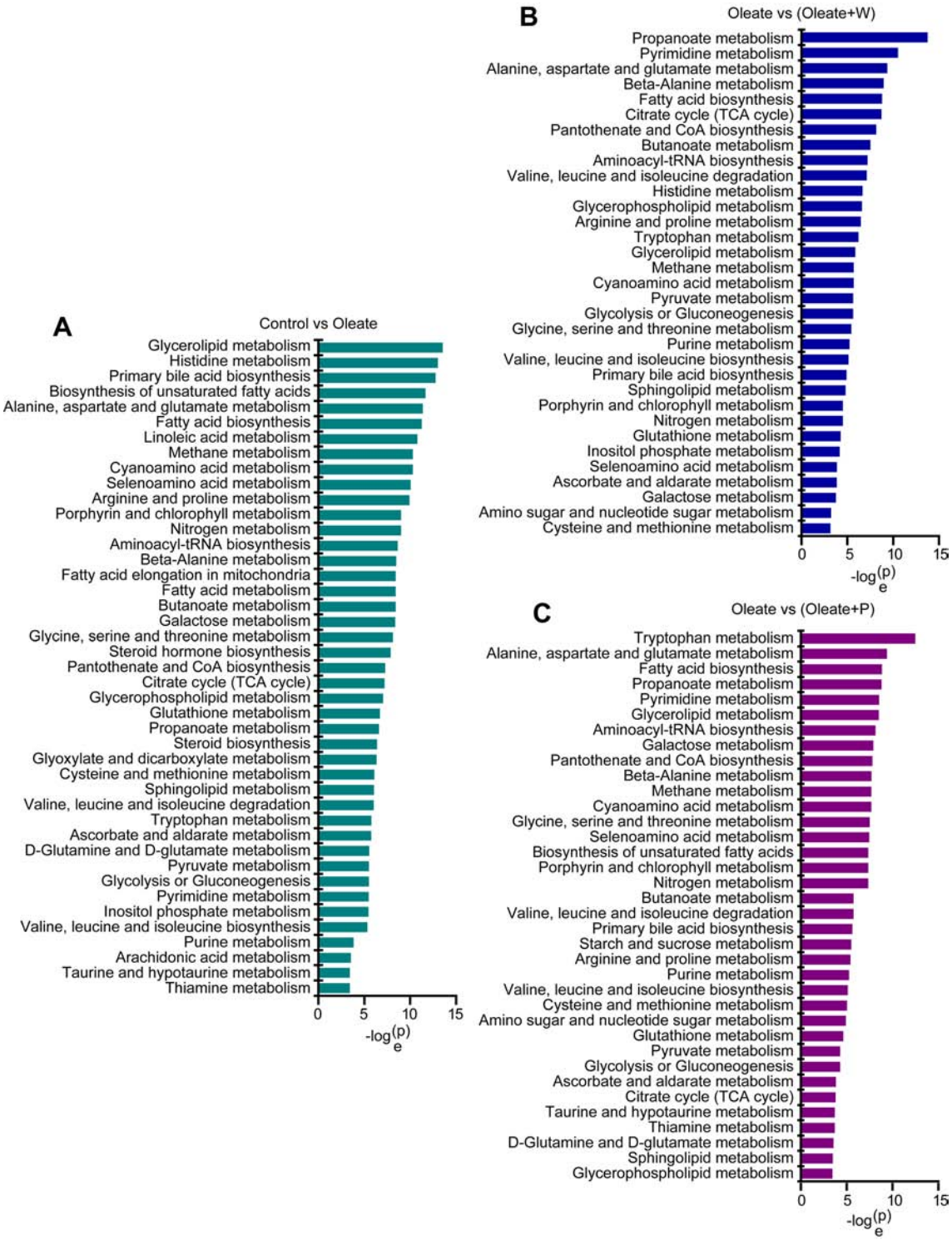

Fig. 3 Changes in metabolic pathways in macrophages treated with oleate, oleate plus WY-14643 (W), and oleate plus pioglitazone (P). Significantly altered metabolic pathways are shown ($p < 0.05$). **a** Changes in metabolic pathways in macrophages treated with oleate. **b** Changes in metabolic pathways in macrophages treated with oleate and oleate plus W. **c** Changes in metabolic pathways in macrophages treated with oleate and oleate plus P

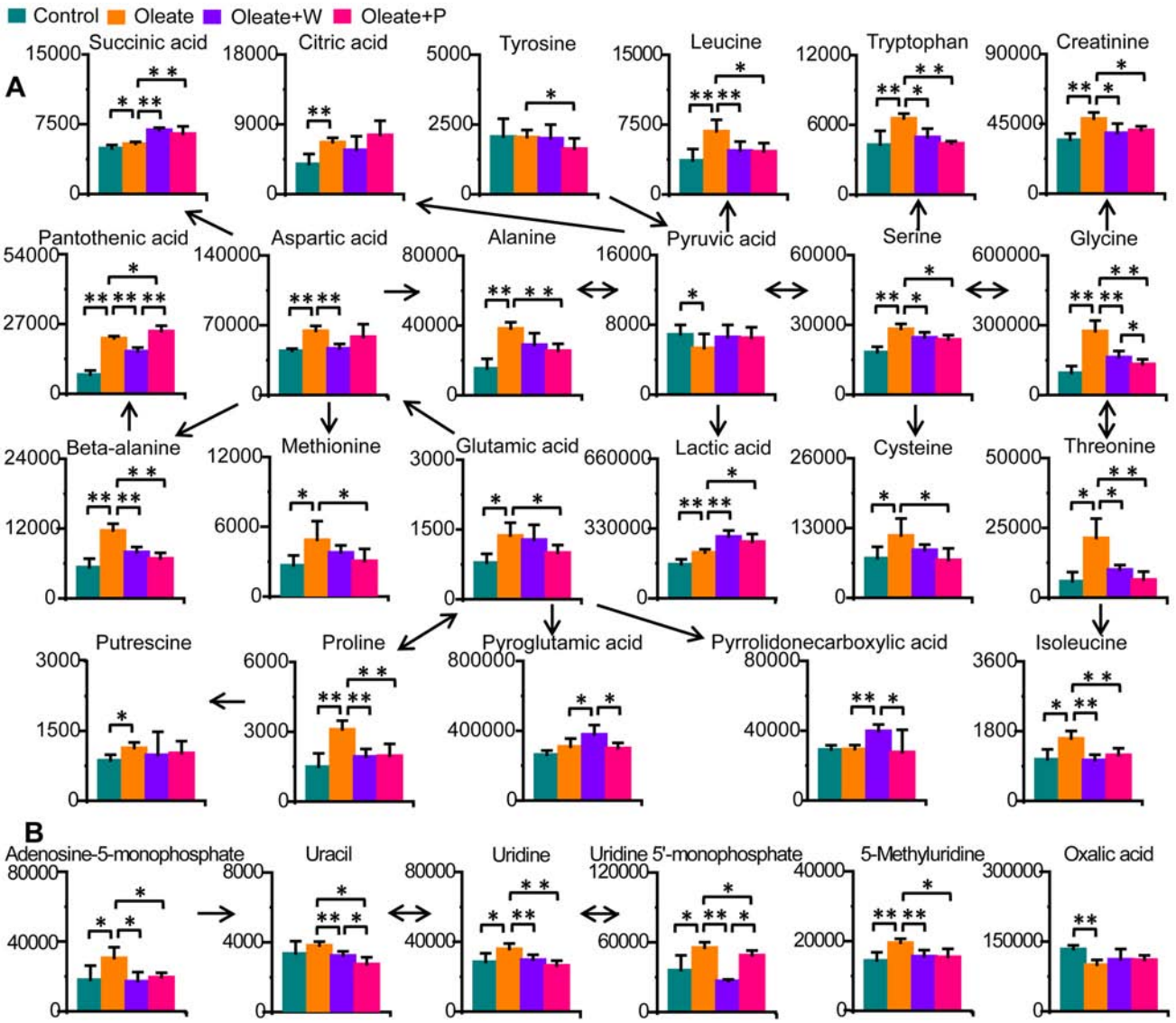

Fig. 4 PPARA/G reprogrammed amino acid metabolism, the tricarboxylic acid cycle and nucleotide metabolism associated with lipid accumulation in macrophages. Columns represent the mean + SD. $^{*}p < 0.05$, $^{**}p < 0.01$, two-tailed Mann–Whitney U test. n = 5 per group. W, WY-14643. P, pioglitazone. PPARA/G reprogrammed amino acid metabolism and the tricarboxylic acid cycle (**a**) and nucleotide metabolism (**b**) associated with lipid accumulation in macrophages

the levels of metabolites involved in amino acid metabolism were attenuated or abolished by PPARA/G activation (Figs. 1, 4a). These data indicate that PPARA/G can effectively reprogramme amino acid metabolism during lipid accumulation in macrophages treated with oleate. Metabolic pathway analysis revealed that the following were significantly altered in macrophages treated with oleate and responsive to PPARA/G activation: alanine, aspartate and glutamate metabolism; glycine, serine and threonine metabolism; valine, leucine and isoleucine biosynthesis/degradation; cysteine and methionine metabolism; arginine and proline metabolism; and tryptophan metabolism (Fig. 3).

PPARA/G activation attenuated oleate-induced increases in alanine, aspartate and glutamate levels in macrophages, which can be attributed to inhibition of alanine–glyoxylate aminotransferase, asparagine synthetase, glutamic-oxaloacetic transaminase, glutamate dehydrogenase and glutaminase (Kersten et al. 2001). Suppression of PPARA/G signaling by oleate in macrophages promoted the deamination and transamination involved in alanine, aspartate and glutamate metabolism, which led to enhanced production of glutamate and aspartate for the synthesis of other amino acids, proteins, lipids, nucleotides and intermediates in the tricarboxylic acid cycle. Levels of glycine, serine and threonine were also significantly increased in macrophages treated

with oleate, and these effects were significantly alleviated by PPARA/G activation. Alanine–glyoxylate aminotransferase is involved in transamination and deamination in glycine, serine and threonine metabolism, and hydroxypyruvate/glyoxylate reductase provides more carbon sources from glucose for serine synthesis. Therefore, accumulation of glycine, serine and threonine in macrophages treated with oleate is likely due to accelerated synthesis via activation of alanine-glyoxylate aminotransferase and hydroxypyruvate/glyoxylate reductase due to PPARA/G suppression by oleate. Accumulation of glycine, serine and threonine suggested more materials for methylation and de novo nucleotide synthesis (Jain et al. 2012; Kersten et al. 2001). Clinical data show that the level of alanine-glyoxylate aminotransferase is significantly associated with risk factors for cardiovascular disease, such as apolipoprotein B, low density lipoprotein (LDL), very low-density lipoprotein, the percentage of small dense LDL, LDL-cholesterol and TGs (Lorenzo et al. 2013; Siddiqui et al. 2013).

We also found that leucine and isoleucine contents were significantly elevated in macrophages treated with oleate and that these effects were alleviated or abolished by PPARA/G activation. Accumulated branched-chain amino acids directly suppress respiration in isolated cardiac mitochondria Complex I and cause disturbances in myocardial redox homeostasis, the hexosamine biosynthetic pathway, lipid metabolism and glucose and pyruvate utilization (Li et al. 2017; Sun et al. 2016). Serum branched-chain amino acids are also elevated in patients with cardiovascular disease and correlate positively with carotid intima-media thickness (Ussher et al. 2016; Yang et al. 2015). Additionally, a 12-year follow-up study revealed that a high score based on branched-chain and aromatic amino acids (isoleucine, phenylalanine and tyrosine) was associated with a higher risk of diabetes and cardiovascular disease (Magnusson et al. 2013). In our study, the level of tryptophan was significantly enhanced in macrophages treated with oleate, and this effect was ameliorated or abolished by PPARA/G signaling activation. The increased level of tryptophan in macrophages treated with oleate might be due to defective metabolism of this amino acid. Treatment with 3-hydroxyanthranilic acid, a metabolite of tryptophan, significantly suppresses oxidized LDL uptake by macrophages and decreases plasma levels of TGs and cholesterol and aortic lesion size in $LDLR^{-/-}$ mice (Zhang et al. 2012) and the urinary ratio of kynurenine to tryptophan has been correlated with adverse prognosis in patients with cardiovascular disease (Pedersen et al. 2013).

Levels of cysteine and methionine were significantly increased in macrophages treated with oleate, and these effects were eliminated by PPARG activation. Elevated cysteine, glycine and glutamine in macrophages treated with oleate indicate more precursors for glutathione synthesis, which is conducive to combating oxidative damage. Increased levels of methionine suggest that PPARG-mediated metabolic reprogramming is correlated with methylation in macrophages (Wijekoon et al. 2005). Additionally, proline and beta-alanine contents were significantly increased in macrophages treated with oleate, and these effects were alleviated or abolished by PPARA/G activation. In a previous study, integrated genetic and metabolic profiling revealed high heritability among amino acids (including proline, arginine, ornithine, alanine, valine and phenylanine) in 117 individuals with premature coronary artery disease (Shah et al. 2009).

Beta-alanine accumulation disturbs energy metabolism and induces oxidative stress (Gemelli et al. 2018). We observed that PPARA/G activation was able to attenuate beta-alanine accumulation in macrophages treated with oleate. Pantothenate, produced from beta-alanine, is the precursor of coenzyme A, which is involved in the metabolism of lipids, proteins and carbohydrates. The level of pantothenate, was significantly elevated in macrophages treated with oleate, and this effects was attenuated by PPARA activation. It has been reported that pantothenate combined with guanidinoacetate and glutamate can predict the development of albuminuria, an effective indicator of cardiovascular disease (Gonzalez-Calero et al. 2016).

3.4 PPARA/G reprogrammes nucleotide metabolism associated with lipid accumulation in macrophages

Nucleotides have vital biological functions, such as energy homeostasis, signal transduction, and RNA and DNA synthesis. We found that levels of adenosine 5-monophosphate, uridine, uridine 5-monophosphate and 5-methyluridine were significantly increased in macrophages treated with oleate and that these effects were alleviated or abolished by PPARA/G activation (Figs. 1, 4b). Additionally, PPARA/G activation reduced the level of uracil in oleate-treated macrophages (Figs. 1, 4b). These data demonstrate that PPARA/G can effectively reprogramme purine and pyrimidine nucleotide metabolism during lipid accumulation in macrophages treated with oleate.

The significant increases observed in the levels of metabolites involved in purine and pyrimidine nucleotide metabolism are likely due to disordered synthesis, hydrolysis, deamination, oxidation, and/or transport in macrophages treated with oleate. PPARA/G transcriptionally controls the synthesis and catabolism of nucleotides, thereby mediating nucleotide homeostasis (Fustin et al. 2012; Kanemitsu et al. 2017; Liu et al. 2013). Xanthine oxidase depletion leads to accumulation of xanthine, hypoxanthine and TGs in renal tubules, contributing to renal interstitial fibrosis in mice (Ohtsubo et al. 2009). Increases in adenosine 5-monophosphate, adenosine, adenine, guanosine and guanosine

monophosphate related to lipid accumulation in adipocyte differentiation have also been observed (Du et al. 2018). Nonetheless, uridine administration was reported to reduce insulin signaling and promote gluconeogenesis, leading to systemic glucose intolerance and a more than three-fold increase in liver lipid content in mice (Urasaki and Pizzorno 2016). Moreover, degradation of 5′-nucleotides (such as guanosine 5′-triphosphate and adenosine 5′-triphosphate) in cardiac myocytes is a distinguishing molecular event in myocardial ischemia (Geisbuhler 2008). Accordingly, disturbed nucleotide metabolism is highly correlated with lipid accumulation in macrophages and cardiovascular disease.

3.5 PPARA/G reprogrammes lipid metabolism associated with lipid accumulation in macrophages

FFAs are involved in various biological functions, such as energy homeostasis and the synthesis of other lipids, i.e., eicosanoids, glycrolipids, CEs, glycerophospholipids and sphingolipids, which are correlated with lipid accumulation. In this study, we found that levels of most FFAs, including palmitate, stearate, palmitoleate, linoleate and arachidonate, were significantly decreased in macrophages treated with oleate but that levels of oleate, 11-eicosenoate and 5,8,11-eicosatrienoate were significantly increased (Fig. 5a). Regardless, PPARA/G activation could not effectively alleviate individual FFA alterations in response to oleate treatment. Considering that each FFA was detected after capillary column and mass spectrum separation and that there were great differences between FFA levels, it is inappropriate to determine total FFAs by directly summing the levels of all FFAs. As described above, the level of total FFAs was significantly increased by oleate in macrophages, and this effect was alleviated by PPARA/G activation. These data suggest disturbances in the transport, oxidation, synthesis of FFAs and/or lipolysis in oleate-treated macrophages, as mediated by PPARA/G. Moreover, monoglyceride levels were significantly increased in oleate-treated macrophages, but these effects were not effectively reversed by PPARA/G activation (Fig. 5b). Alterations in the levels of steroids in macrophages treated with oleate, oleate plus WY-14643, and oleate plus pioglitazone were also observed (Fig. 5c).

3.6 PPARA/G reprogrammes other metabolic pathways associated with lipid accumulation in macrophages

A disordered tricarboxylic acid cycle was also observed in this study. Levels of succinate and citrate were significantly elevated in macrophages treated with oleate, and these effects were aggravated by PPARA/G activation. Succinate accumulation stimulates hypoxia-inducible factor-1α expression, and then enhances interleukin 1β production, which exacerbates the pro-inflammatory status in macrophages (Appari et al. 2018). Furthermore, excessive citrate promotes the generation of pro-inflammatory mediators in macrophages, such as reactive oxygen species, nitric oxide and prostaglandins (O'Neill et al. 2016; O'Neill and Pearce 2016).

Carbohydrate metabolism was also significantly disturbed in macrophages treated with oleate, oleate plus WY-14643, and oleate plus pioglitazone (Fig. S1). After treatment of macrophages with oleate, levels of mannobiose, myo-inositol and scyllo-inositol were significantly increased, and these effects were attenuated or abolished by PPARA/G activation. In contrast, phosphate contents were significantly decreased in macrophages treated with oleate, and this effect was alleviated by PPARA/G activation. These data demonstrate that PPARA/G can effectively reprogramme inositol phoshate metabolism in oleate-treated macrophages. Other metabolic changes in response to treatment with oleate, oleate plus WY-14643, and oleate plus pioglitazone are presented in Fig. S1.

3.7 Potential biomarkers indicative of lipid accumulation and intervention effects of PPARA/G

As described above, the levels of most metabolites involved in amino acid metabolism and nucleotide metabolism were significantly increased in oleate-treated macrophages, and these effects were significantly attenuated or even abolished by PPARA/G activation. As these metabolic changes are indicative of lipid accumulation and the lipid-lowering effects of PPARA/G in macrophages treated with oleate, correlations of the above metabolites with lipids and genes related to PPARA/G signaling were further explored. We found a significantly positive correlation of glycine and tryptophan with neutral lipids, total FFAs, TGs, TC and CE, though glycine and tryptophan were negatively correlated with expression of genes related to PPARA/G signaling (such as *Pparga, Rxra, Ppparg, Rxrg* and *Ppargc1a)* in macrophages after treatment with oleate, oleate plus WY-14643, and oleate plus pioglitazone (Fig. 6a and Tables S2–S4). Owing to the low abundance of tryptophan, only glycine was utilized as a potential biomarker to assess lipid accumulation and the lipid-lowering effects of PPARA/G in oleate-treated macrophages in a binary logistic regression model. Demonstrating good performance and the suitability of glycine as a potential biomarker for assessing lipid accumulation and the lipid-lowering effects of PPARA/G, 100.0% of macrophages treated with oleate, oleate plus WY-14643, and oleate plus pioglitazone were effectively identified (Fig. 6b). After treatment with oleate, oleate plus WY-14643, and oleate

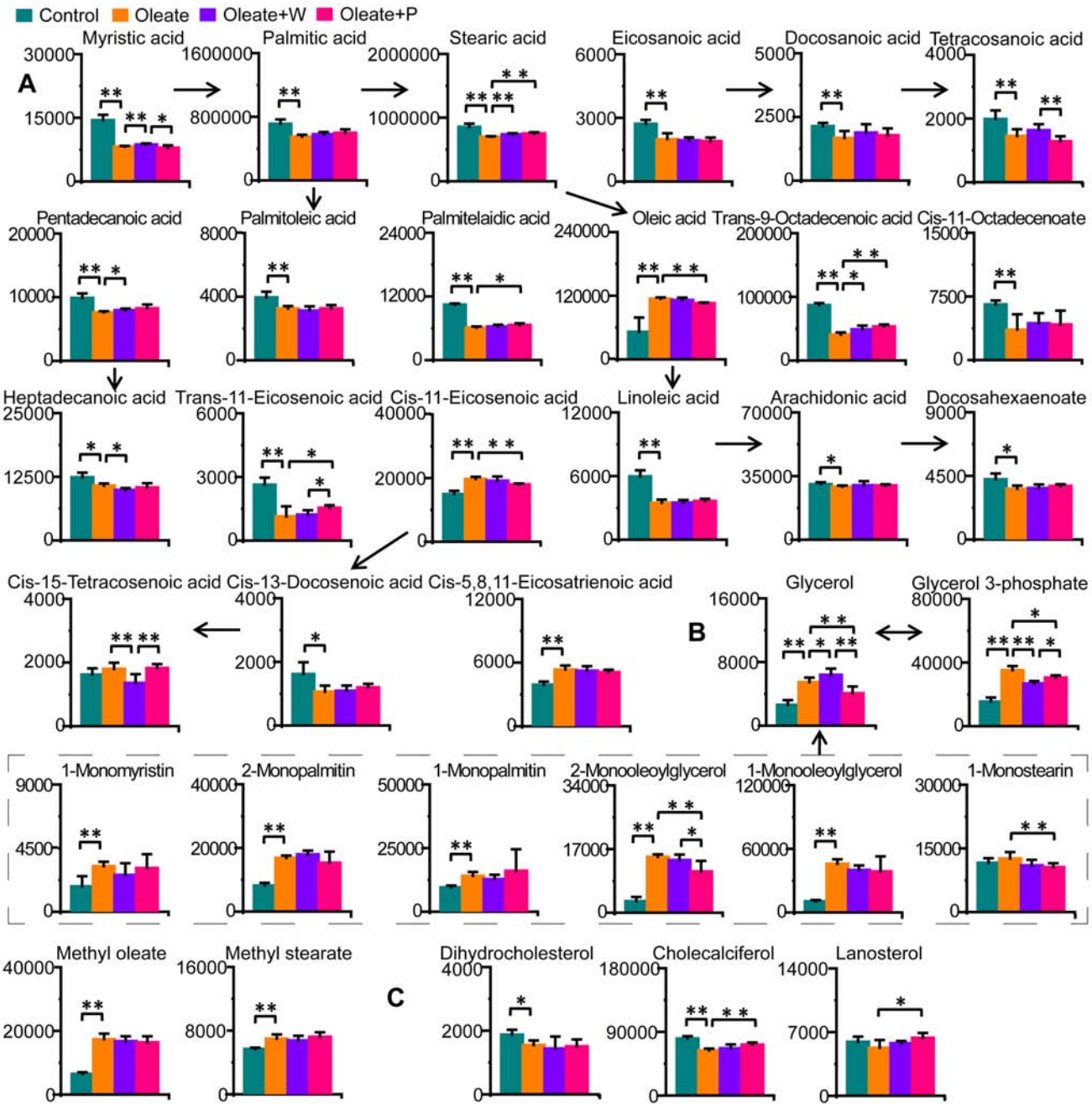

Fig. 5 PPARA/G reprogrammed FFA metabolism, glycerolipid metabolism, and steroid metabolism associated with lipid accumulation in macrophages. Columns represent the mean + SD. $^{*}p < 0.05$, $^{**}p < 0.01$, two-tailed Mann–Whitney *U* test. n = 5 per group. W, WY-14643. P, pioglitazone. PPARA/G reprogrammed FFA (**a**), glycerolipid (**b**) and steroid (**c**) metabolism associated with lipid accumulation in macrophages

plus pioglitazone, an additional batch of macrophage samples were collected to determine the applicability of glycine as a potential biomarker for evaluating lipid accumulation and the lipid-lowering effects of PPARA/G in oleate-treated macrophages. As expected, 100.0% of macrophages treated with oleate, oleate plus WY-14643, and oleate plus pioglitazone were also effectively determined (Fig. 6c). Notably, the application of metabolites as potential biomarkers are affected by specific cells, tissues, organs, environmental stimulus, genetic modifications, physiological status and other factors, which should be paid attention.

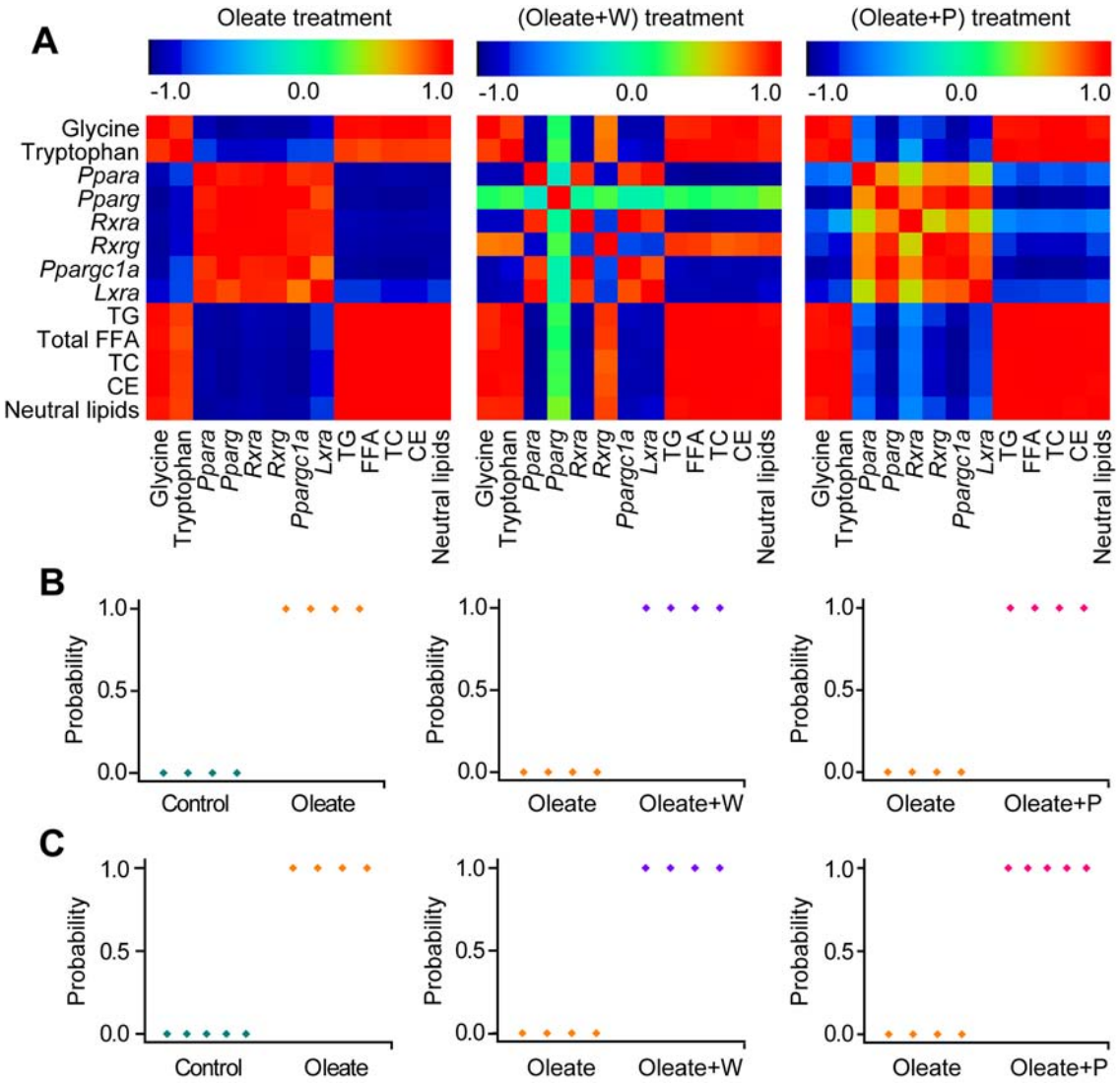

Fig. 6 Potential biomarkers indicative of lipid accumulation and intervention effects of PPARA/G. W, WY-14643. P, pioglitazone. **a** Heat map of correlations of glycine and tryptophan with lipids and genes related to PPAR signaling in response to treatment with oleate, oleate plus W and oleate plus P. Glycine was used as a potential biomarker to evaluate lipid accumulation and the lipid-lowering effects of PPARA/G in macrophages using a binary logistic regression model in the first (**b**) and second (**c**) batch of macrophage samples. The cut-off value was 0.5. (**a, b**), n = 4 per group. **c** n = 5, 4, 4 and 5 in the control, oleate, oleat plus W and oleate plus P group, respectively

4 Conclusions

An untargeted metabolomics approach based on GC–MS was employed to characterize PPARA/G-mediated metabolic reprogramming associated with lipid accumulation in macrophages and the relevant lipid-lowering effects of PPARA/G. We discovered multiple metabolic pathways to be altered during lipid accumulation in oleate-treated macrophages and responsive to oleate plus WY-14643 and oleate plus pioglitazone treatment. Notably, most metabolites involved in amino acid metabolism and nucleotide metabolism accumulated in macrophages treated with oleate, and these effects were alleviated or abolished by PPARA/G activation. Additionally, glycine and tryptophan contents in macrophages were positively correlated with those of neutral lipids, TC, CE, total FFAs and TGs but negatively correlated with expression of genes related to PPARA/G signaling during oleate-triggered lipid accumulation and lipid lowering with WY-14643 and pioglitazone. Furthermore, glycine was proved to be a potential biomarker for evaluating lipid accumulation and the lipid-lowering effects of PPARA/G in oleate-treated macrophages after verification with another independent macrophage sample. The results of this study demonstrate the high correlation of amino acid metabolism (such as glycine, serine and threonine metabolism) with lipid-lowering effects of PPARA/G in macrophages,

suggesting amino acid metabolism as the potential therapeutic target for metabolic diseases.

Acknowledgements This work was supported by the National Natural Science Foundation of China (Nos. 21507128, 41390240, 21777158, 21477124 and 21677140); the Natural Science Foundation of Fujian Province, China (No. 2018J01020); the Key Laboratory of Urban Environment and Health, Institute of Urban Environment, Chinese Academy of Sciences (No. J008); and the Science and Technology Program of Fujian Province, China (No. 2016T3005).

Author contributions GZ and SD conceived and designed this study. GZ performed the instrumental analysis and data processing for metabolomics analysis and subsequent statistical analysis, wrote and revised the manuscript. HG performed the cell experiment and Nile red staining, and detected levels of total FFAs, FC, TC, CE and mRNA expression. YL, DD and YC performed the cell sample preparation for metabolomics analysis. XL and HZ initiated the instrumental analysis.

Compliance with ethical standards

Competing interests The authors declare that they have no conflict of interest.

References

Appari, M., Channon, K. M., & McNeill, E. (2018). Metabolic regulation of adipose tissue macrophage function in obesity and diabetes. *Antioxid Redox Signal, 29*, 297–312.

Barquera, S., Pedroza-Tobias, A., Medina, C., Hernandez-Barrera, L., Bibbins-Domingo, K., Lozano, R., et al. (2015). Global overview of the epidemiology of atherosclerotic cardiovascular disease. *Archives of Medical Research, 46*, 328–338.

Bastien, M., Poirier, P., Lemieux, I., & Despres, J. P. (2014). Overview of epidemiology and contribution of obesity to cardiovascular disease. *Progress in Cardiovascular Diseases, 56*, 369–381.

Bhupathiraju, S. N., & Hu, F. B. (2016). Epidemiology of obesity and diabetes and their cardiovascular complications. *Circulation Research, 118*, 1723–1735.

Du, D., Gu, H., Djukovic, D., Bettcher, L., Gong, M., Zheng, W., et al. (2018). Multiplatform metabolomics investigation of antiadipogenic effects on 3T3-L1 adipocytes by a potent diarylheptanoid. *Journal of Proteome Research, 17*, 2092–2101.

Fustin, J. M., Doi, M., Yamada, H., Komatsu, R., Shimba, S., & Okamura, H. (2012). Rhythmic nucleotide synthesis in the liver: Temporal segregation of metabolites. *Cell Reports, 1*, 341–349.

Geeraerts, X., Bolli, E., Fendt, S.-M., & Van Ginderachter, J. A. (2017). Macrophage metabolism as therapeutic target for cancer, atherosclerosis, and obesity. *Frontiers in Immunology, 8*, 289.

Geisbuhler, T. P. (2008). Compartmentalization of non-adenine nucleotides in anoxic cardiac myocytes. *Basic Research in Cardiology, 103*, 31–40.

Gemelli, T., de Andrade, R. B., Rojas, D. B., Zanatta, A., Schirmbeck, G. H., Funchal, C., et al. (2018). Chronic exposure to beta-alanine generates oxidative stress and alters energy metabolism in cerebral cortex and cerebellum of Wistar rats. *Molecular Neurobiology, 55*, 5101–5110.

Gonzalez-Calero, L., Martin-Lorenzo, M., Martinez, P. J., Baldan-Martin, M., Ruiz-Hurtado, G., Segura, J., et al. (2016). Hypertensive patients exhibit an altered metabolism. A specific metabolite signature in urine is able to predict albuminuria progression. *Translational Research, 178*, 25–37.

Jain, M., Nilsson, R., Sharma, S., Madhusudhan, N., Kitami, T., Souza, A. L., et al. (2012). Metabolite profiling Identifies a key role for glycine in rapid cancer cell proliferation. *Science, 336*, 1040–1044.

Kanemitsu, T., Tsurudome, Y., Kusunose, N., Oda, M., Matsunaga, N., Koyanagi, S., et al. (2017). Periodic variation in bile acids controls circadian changes in uric acid via regulation of xanthine oxidase by the orphan nuclear receptor PPARalpha. *Journal of Biological Chemistry, 292*, 21397–21406.

Kaplan, M., Aviram, M., & Hayek, T. (2012). Oxidative stress and macrophage foam cell formation during diabetes mellitus-induced atherogenesis: Role of insulin therapy. *Pharmacology and Therapeutics, 136*, 175–185.

Kersten, S., Mandard, S., Escher, P., Gonzalez, F. J., Tafuri, S., Desvergne, B., et al. (2001). The peroxisome proliferator-activated receptor alpha regulates amino acid metabolism. *FASEB Journal, 15*, 1971–1978.

Li, T., Zhang, Z., Kolwicz, S. C. Jr., Abell, L., Roe, N. D., Kim, M., et al. (2017). Defective branched-chain amino acid catabolism disrupts glucose metabolism and sensitizes the heart to ischemia-reperfusion injury. *Cell Metabolism, 25*, 374–385.

Liu, Y., Yan, X., Mao, G., Fang, L., Zhao, B., Tang, H., et al. (2013). Metabonomic profiling revealed an alteration in purine nucleotide metabolism associated with cardiac hypertrophy in rats treated with thiazolidinediones. *Journal of Proteome Research, 12*, 5634–5641.

Lorenzo, C., Hanley, A. J., Rewers, M. J., & Haffner, S. M. (2013). The association of alanine aminotransferase within the normal and mildly elevated range with lipoproteins and apolipoproteins: The Insulin Resistance Atherosclerosis Study. *Diabetologia, 56*, 746–757.

Magnusson, M., Lewis, G. D., Ericson, U., Orho-Melander, M., Hedblad, B., Engstrom, G., et al. (2013). A diabetes-predictive amino acid score and future cardiovascular disease. *European Heart Journal, 34*, 1982–1989.

Mandard, S., Muller, M., & Kersten, S. (2004). Peroxisome proliferator-activated receptor alpha target genes. *Cellular and Molecular Life Sciences, 61*, 393–416.

Mathis, D., & Shoelson, S. E. (2011). Immunometabolism: An emerging frontier. *Nature Reviews Immunology, 11*, 81–83.

O'Neill, L. A. J., Kishton, R. J., & Rathmell, J. (2016). A guide to immunometabolism for immunologists. *Nature Reviews Immunology, 16*, 553–565.

O'Neill, L. A. J., & Pearce, E. J. (2016). Immunometabolism governs dendritic cell and macrophage function. *Journal of Experimental Medicine, 213*, 15–23.

Ohtsubo, T., Matsumura, K., Sakagami, K., Fujii, K., Tsuruya, K., Noguchi, H., et al. (2009). Xanthine oxidoreductase depletion induces renal interstitial fibrosis through aberrant lipid and purine accumulation in renal tubules. *Hypertension, 54*, 868–876.

Olefsky, J. M., & Glass, C. K. (2010). Macrophages, inflammation, and insulin resistance. *Annual Review of Physiology, 72*, 219–246.

Pedersen, E. R., Svingen, G. F., Schartum-Hansen, H., Ueland, P. M., Ebbing, M., Nordrehaug, J. E., et al. (2013). Urinary excretion of kynurenine and tryptophan, cardiovascular events, and mortality after elective coronary angiography. *European Heart Journal, 34*, 2689–2696.

Piche, M. E., Poirier, P., Lemieux, I., & Despres, J. P. (2018). Overview of epidemiology and contribution of obesity and body fat distribution to cardiovascular disease: An update. *Progress in Cardiovascular Diseases, 61*, 103–113.

Saeed, A. I., Bhagabati, N. K., Braisted, J. C., Liang, W., Sharov, V., Howe, E. A., et al. (2006). TM4 microarray software suite. *Methods in Enzymology, 411*, 134–193.

Shah, S. H., Hauser, E. R., Bain, J. R., Muehlbauer, M. J., Haynes, C., Stevens, R. D., et al. (2009). High heritability of metabolomic

profiles in families burdened with premature cardiovascular disease. *Molecular Systems Biology, 5*, 258.

Shao, Y., Ye, G., Ren, S., Piao, H. L., Zhao, X., Lu, X., et al. (2018). Metabolomics and transcriptomics profiles reveal the dysregulation of the tricarboxylic acid cycle and related mechanisms in prostate cancer. *International Journal of Cancer, 143*, 396–407.

Siddiqui, M. S., Sterling, R. K., Luketic, V. A., Puri, P., Stravitz, R. T., Bouneva, I., et al. (2013). Association between high-normal levels of alanine aminotransferase and risk factors for atherogenesis. *Gastroenterology, 145*, 1271–1279.

Smith, C. A., Want, E. J., O'Maille, G., Abagyan, R., & Siuzdak, G. (2006). XCMS: Processing mass spectrometry data for metabolite profiling using nonlinear peak alignment, matching, and identification. *Analytical Chemistry, 78*, 779–787.

Sun, H., Olson, K. C., Gao, C., Prosdocimo, D. A., Zhou, M., Wang, Z., et al. (2016). Catabolic defect of branched-chain amino acids promotes heart failure. *Circulation, 133*, 2038–2049.

Urasaki, Y., Pizzorno, G., & Le T. T. (2016). Chronic uridine administration induces fatty liver and pre-diabetic conditions in mice. *PLoS ONE, 11*, e0146994.

Ussher, J. R., Elmariah, S., Gerszten, R. E., & Dyck, J. R. (2016). The emerging role of metabolomics in the diagnosis and prognosis of cardiovascular disease. *Journal of the American College of Cardiology, 68*, 2850–2870.

Wijekoon, E. P., Hall, B., Ratnam, S., Brosnan, M. E., Zeisel, S. H., & Brosnan, J. T. (2005). Homocysteine metabolism in ZDF (type 2) diabetic rats. *Diabetes, 54*, 3245–3251.

Willson, T. M., Lambert, M. H., & Kliewer, S. A. (2001). Peroxisome proliferator-activated receptor gamma and metabolic disease. *Annual Review of Biochemistry, 70*, 341–367.

Xia, J., Sinelnikov, I. V., Han, B., & Wishart, D. S. (2015). MetaboAnalyst 3.0-making metabolomics more meaningful. *Nucleic Acids Research, 43*, W251–W257.

Yang, R. Y., Wang, S. M., Sun, L., Liu, J. M., Li, H. X., Sui, X. F., et al. (2015). Association of branched-chain amino acids with coronary artery disease: A matched-pair case-control study. *Nutrition Metabolism and Cardiovascular Diseases, 25*, 937–942.

Ye, G., Liu, Y., Yin, P., Zeng, Z., Huang, Q., Kong, H., et al. (2014). Study of induction chemotherapy efficacy in oral squamous cell carcinoma using pseudotargeted metabolomics. *Journal of Proteome Research, 13*, 1994–2004.

Ye, G., Zhu, B., Yao, Z., Yin, P., Lu, X., Kong, H., et al. (2012). Analysis of urinary metabolic signatures of early hepatocellular carcinoma recurrence after surgical removal using gas chromatography–mass spectrometry. *Journal of Proteome Research, 11*, 4361–4372.

Zhang, L., Ovchinnikova, O., Jonsson, A., Lundberg, A. M., Berg, M., Hansson, G. K., et al. (2012). The tryptophan metabolite 3-hydroxyanthranilic acid lowers plasma lipids and decreases atherosclerosis in hypercholesterolaemic mice. *European Heart Journal, 33*, 2025–2034.

Zheng, Y., Ley, S. H., & Hu, F. B. (2018). Global aetiology and epidemiology of type 2 diabetes mellitus and its complications. *Nature Reviews Endocrinology, 14*, 88–98.